

# Comparison of the CYP3A Selective Inhibitors CYP3cide, Clobetasol, and Azamulin for Their Potential to Distinguish CYP3A7 Activity in the Presence of CYP3A4/5<sup>S</sup>

Hannah M. Work, Sylvie E. Kandel, and  Jed N. Lampe

Department of Pharmaceutical Sciences, University of Colorado, Anschutz Medical Campus, Skaggs School of Pharmacy and Pharmaceutical Sciences, Aurora, Colorado (H.M.W., S.E.K., J.N.L.)

Received March 5, 2024; accepted April 25, 2024

## ABSTRACT

The CYP3A7 enzyme accounts for ~50% of the total cytochrome P450 (P450) content in fetal and neonatal livers and is the predominant P450 involved in neonatal xenobiotic metabolism. Additionally, it is a key player in healthy birth outcomes through the oxidation of dehydroepiandrosterone (DHEA) and DHEA-sulfate. The amount of the other hepatic CYP3A isoforms, CYP3A4 and CYP3A5, expressed in neonates is low but highly variable, and therefore the activity of individual CYP3A isoforms is difficult to differentiate due to their functional similarities. Consequently, a better understanding of the contribution of CYP3A7 to drug metabolism is essential to identify the risk that drugs may pose to neonates and developing infants. To distinguish CYP3A7 activity from CYP3A4/5, we sought to further characterize the selectivity of the specific CYP3A inhibitors CYP3cide, clobetasol, and azamulin. We used three substrate probes, dibenzylfluorescein, luciferin-PPXE, and midazolam, to determine the IC<sub>50</sub> and metabolism-dependent inhibition (MDI) properties of the CYP3A inhibitors. Probe selection had a significant effect

on the IC<sub>50</sub> values and P450 inactivation across all inhibitory compounds and enzymes. CYP3cide and azamulin were both identified as MDIs and were most specific for CYP3A4. Contrary to previous reports, we found that clobetasol propionate (CP) was not an MDI of CYP3A5 but was more selective for CYP3A5 over CYP3A4/7. We further investigated CYP3cide and CP's ability to differentiate CYP3A7 activity in an equal mixture of recombinant CYP3A4, CYP3A5, and CYP3A7, and our results provide confidence of CYP3cide's and CP's ability to distinguish CYP3A7 activity in the presence of the other CYP3A isoforms.

## SIGNIFICANCE STATEMENT

These findings provide valuable insight regarding in vitro testing conditions to investigate the metabolism of new drug candidates and help determine drug safety in neonates. The results presented here also clearly demonstrate the effect that probe selection may have on CYP3A cytochrome P450 inhibition studies.

## Introduction

Cytochrome P450 (P450) enzymes are responsible for the metabolism of many drugs as well as endogenous substrates and environmental toxins. Of the P450 enzymes, the CYP3A subfamily is the most abundant in the liver and metabolizes over 50% of marketed drugs (Shankar and Mehendale, 2014). The CYP3A subfamily consists of four isoforms—CYP3A4, CYP3A5, CYP3A7, and CYP3A43. In the adult liver, CYP3A4 accounts for 10%–50% of the total P450 content, whereas CYP3A5 is highly polymorphic and primarily expressed in individuals of African and Asian descent (Stewart and Hampton, 1987; Maldonado et al., 2017). In general, CYP3A43 is not considered to be significantly involved in drug metabolism, whereas CYP3A7 is predominantly expressed in fetal and neonatal livers, accounting for


~50% of the total hepatic P450 content and 87%–100% of the hepatic CYP3A content (Li and Lampe, 2019). The hepatic expression levels of CYP3A7 have been found to increase until around birth and then begin to rapidly decline. Simultaneously, CYP3A4 expression increases (Zane et al., 2018). This makes expression levels of CYP3A4 and CYP3A7 highly variable during the first month of life. CYP3A5 seems to be consistently expressed but at significantly lower levels than CYP3A4 and CYP3A7 (Leeder et al., 2005; Zane et al., 2018). Thus, CYP3A7 is the predominant CYP3A enzyme expressed during the first month postgestation and therefore contributes an outsized role in the metabolism of CYP3A substrates during this time period (Morselli et al., 1980).

The variability in CYP3A isoform expression can consequently cause changes in the pharmacokinetics and toxicity of a number of prescribed drugs. This, in turn, frequently exposes neonates to potential drug–drug interactions (DDIs) due to the high occurrence of polypharmacy in these patients (Fabiano et al., 2012; Van den Anker et al., 2020). In a cohort study of 220 pediatric patients in the neonatal intensive care unit (NICU), fentanyl administration led to DDIs in 22.3% of neonates admitted to the NICU, causing serious adverse reactions (Costa et al., 2021). In adults, fentanyl is metabolized by CYP3A4; however, the extent to which CYP3A7 metabolizes fentanyl in neonates is unknown.

Funding for this work was generously provided through National Institutes of Health National Institute of Allergy and Infectious Diseases [Grant R01AI183687-01] (to J.N.L.).

No author has an actual or perceived conflict of interest with the contents of this article.

dx.doi.org/10.1124/dmd.124.001598.

 This article has supplemental material available at [dmd.aspetjournals.org](http://dmd.aspetjournals.org).

**ABBREVIATIONS:** 1'-OH-MDZ, 1'-hydroxy midazolam; 4-OH-MDZ, 4-hydroxy midazolam; CE, collision energy; CP, clobetasol propionate; CV, cone voltage; DBF, dibenzylfluorescein; DDI, drug–drug interaction; DHEA, dehydroepiandrosterone; HLM, human liver microsome; IPA, isopropyl acetal; LC-MS/MS, liquid chromatography tandem mass spectrometry; MDI, metabolism-dependent inhibition/inhibitor; MDZ, midazolam; MRM, multiple reaction monitoring; nHLM, neonatal human liver microsome; NICU, neonatal intensive care unit; P450, cytochrome P450.

On average, CYP3A7 has a much slower rate of metabolism and an approximately 10-fold lower turnover rate ( $k_{cat}$ ) for most drug substrates when compared with CYP3A4 (Williams et al., 2002). Pacifici (2015) concluded that the longer half-life and lower rate of fentanyl elimination in neonates is due to the high expression levels of CYP3A7 and low expression levels of CYP3A4. These effects were exacerbated when fentanyl was concurrently administered with midazolam (MDZ) or fluconazole, a substrate and an inhibitor of CYP3A, respectively.

Thus, understanding the contribution of CYP3A7 to drug metabolism is essential to identifying the risk that drugs may pose to neonates and developing infants. Traditionally, the gold standard for assessing drug metabolism is human liver microsomes (HLMs). However, due to structural and amino acid sequence similarities, all CYP3A enzymes have overlapping substrate specificities. Therefore, no single probe exists that can differentiate the activity of these enzyme isoforms. However, recent studies have identified three CYP3A-specific inhibitors: CYP3cide (Walsky et al., 2012), clobetasol propionate (CP) (Wright et al., 2020), and azamulin (Chanteux et al., 2020) (Fig. 1).

Walsky et al. (2012) previously identified CYP3cide to be a mechanism-based inactivator of CYP3A4. A concentration of 0.05  $\mu$ M CYP3cide reportedly inhibited CYP3A4 midazolam hydroxylation by 84%. Similarly, CP is reported to be a selective inhibitor of CYP3A5, with a potent  $IC_{50}$  value roughly 100-fold lower than that of CYP3A4 (0.206  $\mu$ M versus 15.6  $\mu$ M, respectively) based upon testing of recombinant CYP3A enzymes using the substrate luciferin-isopropyl acetal (IPA). However, the effect CP has on CYP3A7 was not investigated nor was its ability to inactivate CYP3A4 or CYP3A5 (Wright et al., 2020). Similarly, azamulin has been reported to be a specific CYP3A4/5 inhibitor, with an  $IC_{50}$  value of  $\sim$ 0.5  $\mu$ M as determined in primary human hepatocytes (Chanteux et al., 2020). However, examination of the individual recombinant CYP3As was not reported, and CYP3A7 was not included in the previous studies (Chanteux et al., 2020).

Herein, we tested all three inhibitors with a variety of substrate probes and measured the effect they have on the activity of CYP3A4, CYP3A5, and CYP3A7 to determine their adequacy in distinguishing CYP3A7 activity. Enzyme activities were assessed using three specific substrate probes—dibenzylfluorescein (DBF) (fluorescence-based assay), luciferin-PPXE (luminescence-based assay), and midazolam [liquid chromatography tandem mass spectrometry (LC-MS/MS)-based assay]. The mixed inhibitor system reported here could be used to reduce off-target inhibitory effects on CYP3A7 to characterize the specific contribution of CYP3A7-mediated metabolism in neonatal HLMs (nHLMs).

### Materials and Methods

**Chemicals and Recombinant Enzymes.** Insect cell microsomes prepared from baculovirus-infected Sf9 cells (Supersomes) expressing human CYP3A4 (catalog #456202), CYP3A5 (catalog #456256), or CYP3A7 (catalog # 456237)

enzymes and insect controls (catalog #456200) were purchased from Corning (Corning, NY). These Supersomes contain recombinant P450 enzyme coexpressed with human NADPH-cytochrome P450 reductase and human cytochrome  $b_5$ . Midazolam (CAS: 59467-70-8) prepared in methanol (1 mg/mL),  $\alpha$ -hydroxymidazolam- $d_4$  prepared in methanol (100  $\mu$ g/mL, catalog #H-921), dehydroepiandrosterone (DHEA)- $d_3$  (CAS:97453-25-3) prepared in methanol (100  $\mu$ g/mL), CYP3cide (catalog #PZ0195), CP (CAS: 25122-46-7), azamulin (CAS: 76530-44-4), 1'-hydroxy-midazolam (1'-OH-MDZ; CAS: 59468-90-5), 4-hydroxy-midazolam (4-OH-MDZ; CAS: 59468-85-8), glucose-6-phosphate, glucose-6-phosphate dehydrogenase, and NADP<sup>+</sup> were all obtained from Sigma-Aldrich (St. Louis, MO). Dibenzylfluorescein (CAS: 97744-44-0) was obtained from Cayman Chemical (Ann Arbor, MI). DHEA (CAS: 53-43-0), 16 $\alpha$ -hydroxy-DHEA (CAS: 1232-73-1), 7 $\alpha$ -hydroxy-DHEA (CAS: 53-00-9), and 7 $\beta$ -hydroxy-DHEA (CAS: 2487-48-1) were purchased from Steraloids (Newport, RI). The P450-Glo CYP3A4 assay kit with luciferin-PPXE (catalog #V8912) was purchased from Promega (Madison, WI); this kit includes the luciferin-PPXE probe and the luciferin detection reagent. All other chemicals and solvents used were obtained from standard suppliers and were of reagent or analytical grade.

**Testing Selectivity of CYP3A Inhibitors and Probe Substrate Effects Using the Nondilution  $IC_{50}$  Method.** Assays were conducted in triplicate in 96-well polystyrene plates: flat black microtiter plates (Corning, catalog #3915) for fluorescent assays, flat white plates (Corning, catalog #3912) for luminescent assays, and clear deep-well plates (Sigma, catalog #BR01352) for liquid chromatography–mass spectrometry assays. The testing conditions and reaction parameters are presented in Supplemental Table 1. To assess time and NADPH dependence, the nondilution method was performed as previously described (Parkinson et al., 2011; <https://www.cyprotex.com/admek/in-vitro-metabolism/cytochrome-p450-tdi-ic50-shif>). In brief, individual CYP3As (2–20 pmol/ml final) and inhibitors were preincubated in the presence and the absence of an NADPH regeneration mixture for 30 minutes at 37 °C before adding the probe substrate ( $\sim K_m$ ) to all wells, and NADPH regeneration mixture (at final concentrations in the incubations of 1 mM NADP<sup>+</sup>, 10 mM glucose-6-phosphate, and 2 IU/mL glucose-6-phosphate dehydrogenase) was added to the reactions not preincubated with NADPH. The reaction buffer consisted of 0.1 M potassium phosphate (Kpi) buffer (pH 7.4) and 3.3 mM magnesium chloride (MgCl<sub>2</sub>). Samples were further incubated with the probe substrate before subsequently stopping the reaction at the indicated timepoints, either by 2 M NaOH (75  $\mu$ l, DBF), luciferin detection reagent (50  $\mu$ l, luciferin-PPXE), or methanol containing 100 ng/mL  $\alpha$ -hydroxymidazolam- $d_4$  internal standard (200  $\mu$ l). Standard-condition  $IC_{50}$  assays were conducted with no 30-minute preincubation step (i.e., 0 minutes preincubation). All assays included incubations without the CYP3A enzyme(s) and were used as negative controls. Incubations with 0.25  $\mu$ M ritonavir (+/– NADPH preincubation) were used as a positive control for inhibition. Inhibitors were prepared at a stock concentration of 30–60 mM in DMSO and serially diluted twofold. DMSO concentrations in vials were kept below 0.1% (v/v). Metabolite formation was measured at an excitation and emission wavelength of 485/538 nm for DBF, and luminescent signal was detected using the Tecan Infinite 200 PRO. For the midazolam assays, plates were centrifuged for 20 minutes at 2000g and 4 °C to precipitate proteins, and 5  $\mu$ l aliquots of the supernatants were analyzed by LC-MS/MS. Metabolites of midazolam (1'-OH- and 4-OH-MDZ) were detected by multiple reaction monitoring (MRM) scans as described below.

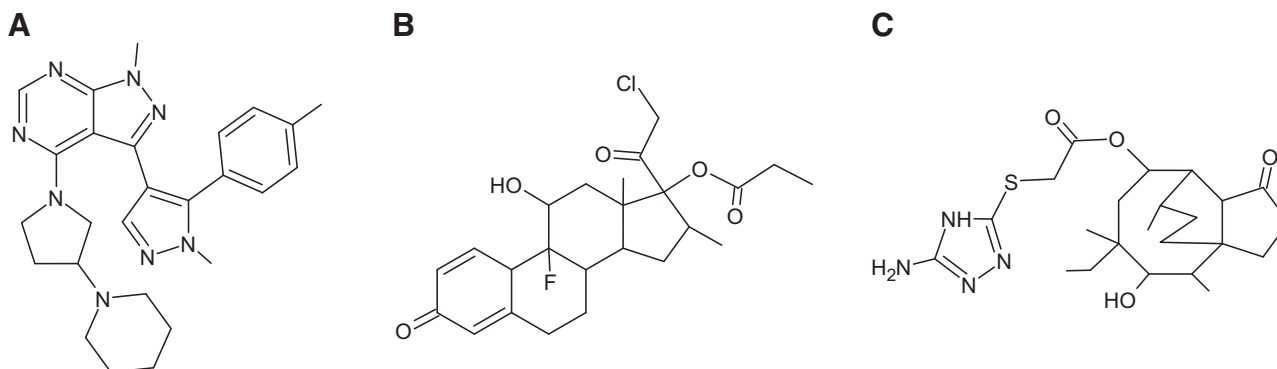


Fig. 1. Chemical structures of (A) CYP3cide, (B) clobetasol propionate, and (C) azamulin.

**Analytical Method for Midazolam Hydroxylation.** The Waters Acquity UPLC system interfaced by electrospray ionization with a Waters Xevo TQ-S micro tandem quadrupole mass spectrometer (Waters Corp., Milford, MA) was used in the positive ionization mode and with the MRM scan type. The following source conditions were applied: 0.5 kV for the capillary voltage, 150°C for the source temperature, 500°C for the desolvation temperature, 0 L/h for the cone gas flow, and 900 L/h for the desolvation gas flow. The following mass transitions, collision energies (CEs), and cone voltages (CVs) were used to detect the respective analytes: 326 > 291 (CE, 28 V; CV, 10 V) for midazolam, 342 > 203 (CE, 28 V; CV, 15 V) for 1'-OH-MDZ, 342 > 234 (CE, 20 V; CV, 25 V) for 4-OH-MDZ, and 346 > 203 (CE, 26; CV, 25 V) for  $\alpha$ -hydroxy-midazolam- $d_4$ , used as the internal standard. Analytes were separated on a Waters BEH C18 column (1.7  $\mu$ m, 2.1  $\times$  50 mm) by flowing 0.1% formic acid in water and methanol at 0.5 mL/min. The following gradient was used: 10% organic (methanol) held for 0.5 minutes, increased to 98% over 2.5 minutes, and held at 98% for 1.0 minutes. The mass spectrometry peaks were integrated using QuanLynx software (version 4.1, Waters Corp.), and the analyte:internal standard peak area ratios were used to quantify the percentage of inhibition compared with the solvent control peak area ratios.

**DHEA Inhibition by CYP3cide and CP in Recombinant CYP3A Mixtures.** Assays were conducted in triplicate in clear deep-well plates (Sigma, catalog #BR01352) with volumes of 200  $\mu$ L. Reactions consisted of 0.1 M Kpi (pH 7.4), 3.3 mM MgCl<sub>2</sub>, and varying mixtures of CYP3A enzymes containing equal amounts of CYP3A enzymes (5 pmol/mL CYP3A7, 5 pmol/ml CYP3A7 and CYP3A4, 5 pmol/ml CYP3A7 and CYP3A5, and 5 pmol/ml CYP3A7, CYP3A4, and CYP3A5). Insect cell control microsomes were added to the incubations to ensure consistency of the protein concentrations between the different CYP3A mixtures. For samples that included CYP3cide (1  $\mu$ M final), CYP3cide and enzyme mixtures were preincubated at 37°C in the presence of NADPH regeneration mixture (1 mM NADP<sup>+</sup>, 10 mM glucose-6-phosphate, and 2 IU/mL glucose-6-phosphate dehydrogenase final) for 30 minutes before adding the probe substrate DHEA (5  $\mu$ M final) or DHEA and CP (5  $\mu$ M and 0.5  $\mu$ M final, respectively) to individual tubes. For reactions only containing CP, enzyme mixtures were preincubated at 37°C for 3 minutes before adding the probe substrate and inhibitor, after which the incubation was started by the addition of NADPH regeneration mix. All incubations were further incubated at 37°C for 8 minutes and then stopped by the addition of 200  $\mu$ L methanol containing 200 ng/mL DHEA- $d_3$  as internal standard. DMSO and methanol concentrations were kept below 0.2% (v/v). Samples were incubated under steady-state kinetic conditions as determined from a prior experiment establishing linearity up to a 20-minute incubation time (data not shown). Incubations without NADPH served as negative controls. Precipitated proteins were collected by centrifugation of the stopped samples for 20 minutes at 2000g and 4°C. Supernatants were transferred to high-performance liquid chromatography vials, and aliquots of 5  $\mu$ L were analyzed by LC-MS/MS. The 7 $\alpha$ -, 7 $\beta$ -, and 16 $\alpha$ -hydroxy-DHEA metabolites were quantified based on a calibration curve ranging from 0.015  $\mu$ M to 3.75  $\mu$ M.

**Analytical Method for Detection of DHEA Hydroxylation.** The Waters Acquity UPLC system, interfaced by electrospray ionization with a Waters Xevo TQ-S micro tandem quadrupole mass spectrometer (Waters Corp.), was used in the positive ionization mode and with the MRM scan type. The following source conditions were applied: 1.0 kV for the capillary voltage, 150°C for the source temperature, 500°C for the desolvation temperature, 50 L/h for the cone gas flow, and 900 L/h for the desolvation gas flow. The following mass transitions, CEs, and CVs were used to detect the respective analytes: 289.3 > 253.25 (CE, 10.0 V, CV, 20.0 V) for DHEA, 287.2 > 211.2 (CE, 18.0 V, CV, 10.0) for 7 $\alpha$ -, 7 $\beta$ - and 16 $\alpha$ -hydroxy DHEA, and 294.2 > 258.2 (CE, 12.0 V, CV, 10.0 V) for DHEA- $d_3$ , used as the internal standard. Analytes were separated on a Waters BEH C18 column (1.7  $\mu$ m, 2.1  $\times$  100 mm) by flowing 0.1% formic acid in water and acetonitrile at 0.4 mL/min. The following gradient was used: 20% organic (acetonitrile) held for 0.5 minutes, increased to 70% over 3.5 minutes, further increased to 98% over 0.5 minutes, and held at 98% for 1 minute. The mass spectrometry peaks were integrated using QuanLynx software (version 4.1, Waters Corp.), and the analyte:internal standard peak area ratios were used to quantify metabolite formation. For determination of the hydroxy metabolite concentrations, the regression fits were based on the analyte:internal standard peak area ratios calculated from the calibration standards, and the analyte concentrations in the incubations were back-calculated using a weighted (1/x) linear least-squares regression.

**Data Analysis.** Inhibition percentages were calculated based on the retrieved signal without inhibitor present (solvent control, 0% inhibition). Data were fitted to a nonlinear regression model [(Inhibitor) versus response (three parameters)] in GraphPad Prism (version 9.5.0), considering only the mean Y value of each point. The bottom and top of the curve were constrained to constants equal to 0 and 100, respectively. For experiments evaluating the effect of NADPH in the preincubation, the best-fit IC<sub>50</sub> values were compared using the extra sum-of-squares *F* test. DHEA metabolism by various CYP3A mixtures was compared with the CYP3A7 control by multiple unpaired *t* tests with Welch correction to account for differences in standard deviation across groups. A *P* value of 0.05 was considered the threshold for significance.

## Results

**CYP3cide Inhibition Selectivity for CYP3A Isoforms.** Examination of recombinant CYP3A4, CYP3A5, and CYP3A7 revealed that CYP3cide was selective for CYP3A4 across all probes tested (Fig. 2; Table 1). Initially, experiments were done to assess the impact of the absence of NADPH in the preincubation reaction. Using DBF as a probe (Fig. 2, A–C), the mean IC<sub>50</sub> values for CYP3A4, CYP3A5, and CYP3A7 were 0.273  $\mu$ M, 27.0  $\mu$ M, and 55.7  $\mu$ M, respectively. Luciferin-PPXE (Fig. 2, D–F) resulted in lower IC<sub>50</sub> values across all enzymes: 0.0960  $\mu$ M, 4.52  $\mu$ M, and 30.4  $\mu$ M for CYP3A4, CYP3A5, and CYP3A7, respectively. Assessment with midazolam (Fig. 2, G–I) generated comparable, albeit slightly increased, IC<sub>50</sub> values as DBF and luciferin across all enzymes, with IC<sub>50</sub> values of 0.119  $\mu$ M, 20.2  $\mu$ M, and 72.8  $\mu$ M for CYP3A4, CYP3A5, and CYP3A7, respectively. Excluding CYP3A5 testing with luciferin-PPXE, these results are consistent with previous reports (Williams et al., 2002; Walsky et al., 2012; Wright et al., 2020).

IC<sub>50</sub> shifts, suggesting metabolism-dependent inhibition (MDI), were only observed in the CYP3A4 experiments, with the exception once again of CYP3A5 and luciferin-PPXE (Fig. 2E); however, the shift observed with CYP3A5/luciferin-PPXE was not statistically significant (*P* = 0.08), and the time/NADPH-dependent IC<sub>50</sub> value (1.94  $\mu$ M) is still 100 times greater than that determined in the CYP3A4 experiments (0.0378  $\mu$ M). CYP3A4 metabolism-dependent IC<sub>50</sub> values were 0.00413  $\mu$ M, 0.0378  $\mu$ M, and 0.0665  $\mu$ M in CYP3A4 experimentation with midazolam, luciferin-PPXE, and DBF, respectively. To account for the effects of nonspecific protein binding, a control experiment adjusting for protein content was conducted to ensure that the significant change in time/NADPH-dependent IC<sub>50</sub> values was not due to nonspecific protein binding in the incubations that could affect the free concentration of the inhibitor (Supplemental Fig. 1). Overall, the CYP3cide IC<sub>50</sub> values for CYP3A4 were at least 100-fold lower compared with CYP3A5 and CYP3A7 across all probe substrates, making this a promising inhibitor for our intended purposes.

**CP Inhibition Selectivity for CYP3A Isoforms.** Our assessment of CP with CYP3A4, CYP3A5, and CYP3A7 demonstrated that the compound was most selective for CYP3A5 inhibition (Fig. 3; Table 2). Across all probes tested, no significant IC<sub>50</sub> shift was measured with CYP3A5, indicating no metabolism dependency for the inhibition observed. Using DBF as a probe (Fig. 3, A–C), CP was at least one order of magnitude more potent at inhibiting CYP3A5 than CYP3A4 and CYP3A7, with IC<sub>50</sub> values of 0.157  $\mu$ M, 9.29  $\mu$ M, and 2.55  $\mu$ M, respectively. Similar inhibition values were observed for CYP3A4 and CYP3A5 when testing with midazolam (Fig. 3, G–I), with IC<sub>50</sub> values of 3.16  $\mu$ M and 0.128  $\mu$ M, respectively. Conversely, CYP3A7 inhibition by CP resulted in reduced inhibitory potency with midazolam (15.83  $\mu$ M) compared with the other probe substrates.

Although activity testing using luciferin-PPXE as a probe did not significantly change the IC<sub>50</sub> value retrieved for CYP3A4 or CYP3A7 (3.16  $\mu$ M and 3.78  $\mu$ M, respectively; Table 2), a significantly different

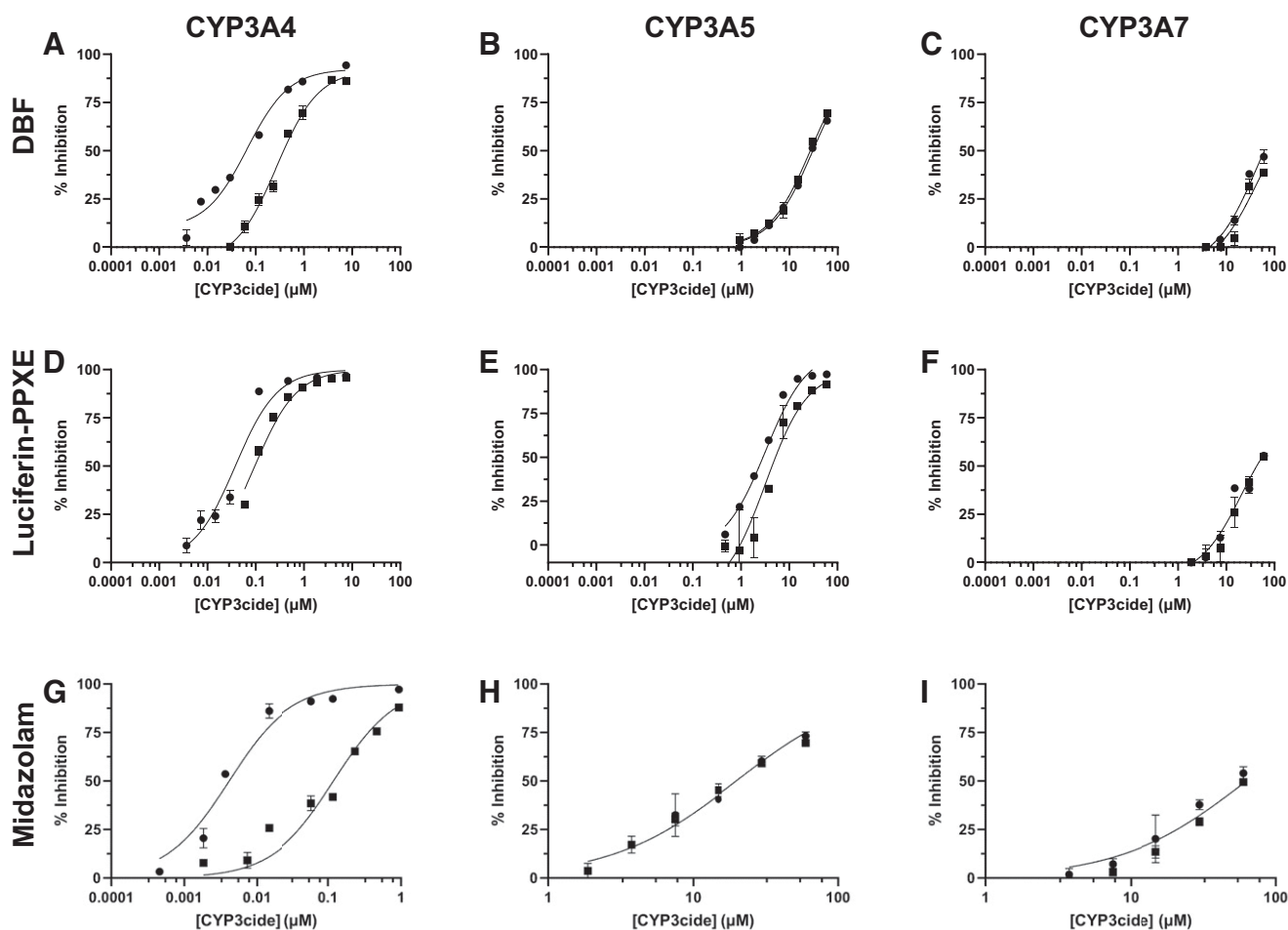


**Fig. 2.** CYP3A4, CYP3A5, and CYP3A7 selectivity for CYP3cide inhibition using dibenzylfluorescein (A–C), luciferin-PPXE (D–F), and midazolam (G–I) as probes. Data points represent the average of triplicate incubations, with error bars representing the standard deviations. Filled circles, 30-minute preincubation in the presence of NADPH; closed squares, 30-minute preincubation in the absence of NADPH. Complete  $IC_{50}$  curves for CYP3A5 and CYP3A7 testing could not be generated due to solubility and DMSO solvent constraints. All curves were generated as described in *Materials and Methods*.

value was observed with CYP3A5. The resulting  $IC_{50}$  value was  $0.0382 \mu\text{M}$  (Fig. 3E). This is most likely due to the poor capabilities of CYP3A5 to metabolize luciferin-PPXE. Upon characterization, we discovered that CYP3A5 was the least catalytically active metabolizer of luciferin-PPXE, requiring higher concentrations of CYP3A5 and the luciferin probe to quantify CYP3A5 activity (Supplemental Fig. 2). Luciferin-PPXE also generated data that did not fit the standard slope equation when testing CYP3A4 inhibition by CP ( $R^2$ , 0.766). Refitting the data to the variable slope equation results in an improved fit (Fig. 3D;  $R^2$ , 0.998) and an  $IC_{50}$  value of  $4.95 \mu\text{M}$  when adjusting the Hill slope from 1.0 to 0.528, suggesting negative cooperativity toward CYP3A4 versus CYP3A5. These results highlight the importance of probe selection on P450 inhibition studies. However, across all probe substrates tested, CP was more selective for CYP3A5 by 1 to 2 orders of magnitude compared with CYP3A4 and CYP3A7. At lower concentrations, CP could possibly be used to inhibit CYP3A5 activity without significantly reducing CYP3A7 activity.

**Azamulin Inhibition Selectivity for CYP3A Isoforms.** Upon testing azamulin for its selectivity, we found that azamulin was most selective for CYP3A4 across all probe substrates tested; however, the value varied based on probe selection (Fig. 4; Table 3). Although  $IC_{50}$  values were similar among all three probes, the metabolism-dependent  $IC_{50}$  differed greatly. No significant  $IC_{50}$  shift was detected with DBF

(Fig. 4A) ( $0.171 \mu\text{M}$  versus  $0.104 \mu\text{M}$ ); however, both luciferin-PPXE (Fig. 4D) and midazolam (Fig. 4G) produced more significant  $IC_{50}$  shifts, albeit to different extents. Using luciferin-PPXE as a probe, the  $IC_{50}$  value shifted from  $0.156 \mu\text{M}$  to  $0.0573 \mu\text{M}$ , a 2.7-fold shift. Midazolam testing produced a 52-fold shift, from  $0.0585 \mu\text{M}$  to  $0.00112 \mu\text{M}$ . A similar pattern was observed with CYP3A7 (Fig. 4, C, F, and I). DBF did not exhibit a significant  $IC_{50}$  shift ( $>1.5$ -fold) resulting from NADPH preincubation with CYP3A7, but it demonstrated a general trend in that direction; the standard-condition and metabolism-dependent  $IC_{50}$  values were  $0.614$  and  $0.427 \mu\text{M}$ , respectively, resulting in a 1.4-fold shift. Luciferin-PPXE and midazolam led to comparable values for CYP3A7,  $1.10 \mu\text{M}$  and  $1.31 \mu\text{M}$ , respectively, and a greater than twofold  $IC_{50}$  shift was observed with these probe substrates.

In contrast to CYP3A4 and CYP3A7, CYP3A5 produced substantially different results across all probe substrates tested. No  $IC_{50}$  shift was observed with either the DBF or midazolam substrate probes; however, the amount of inhibition detected with DBF was approximately twofold less than midazolam, the values being  $1.07$  and  $0.580 \mu\text{M}$ , respectively. On the other hand, luciferin-PPXE did demonstrate an  $IC_{50}$  shift with azamulin from  $2.34 \mu\text{M}$  to  $0.901 \mu\text{M}$ , an approximately 2.6-fold shift. Nevertheless, the time/NADPH-dependent  $IC_{50}$  detected with luciferin-PPXE is comparable to the standard-condition  $IC_{50}$  values detected with midazolam and DBF as probe substrates. Although

TABLE 1  
CYP3cide IC<sub>50</sub> shift for recombinant CYP3A4, CYP3A5, and CYP3A7 enzymes

| Probe Substrate | CYP3cide IC <sub>50</sub> (μM) (95% CI) [R <sup>2</sup> ] |                              |                |                              |                               |            |
|-----------------|---|------------------------------|----------------|------------------------------|-------------------------------|------------|
|                 | DBF   |                              | Luciferin-PPXE |                              | Midazolam                     |            |
|                 | -NADPH preincubation                                      | +NADPH preincubation         | Fold shift     | -NADPH preincubation         | +NADPH preincubation          | Fold shift |
| CYP3A4          | 0.273 (0.16-0.443) [0.99]                                 | 0.0665 (0.0222-0.185) [0.97] | 4.11           | 0.0960 (0.0768-0.119) [0.97] | 0.0378 (0.0259-0.0559) [0.97] | 2.54       |
| CYP3A5          | 27.0 (25.1-29.1) [0.99]                                   | 30.5 (27.7-33.6) [0.99]      | 0.885          | 4.52 (1.80-11.4) [0.97]      | 1.94 (1.12-3.21) [0.99]       | 2.33       |
| CYP3A7          | 55.7 <sup>a</sup> [0.92]                                  | 33.0 <sup>a</sup> [0.97]     | 1.69           | 30.4 <sup>a</sup> [0.99]     | 13.6 <sup>a</sup> [0.95]      | 2.24       |

<sup>a</sup>95% confidence intervals unable to be generated due to incomplete curve (solubility restrictions).

azamulin is referenced to be a specific CYP3A inhibitor, our findings indicate that it is most selective for CYP3A4 and cannot differentiate between CYP3A5 and CYP3A7 activity.

**Selectivity of CYP3cide and CP for CYP3A4/5 Inhibition in a Recombinant CYP3A Mixture.** To differentiate CYP3A7 activity in a recombinant CYP3A mixture that might mimic nHLMs, we selected the inhibitors CYP3cide and CP. Although azamulin was more selective for CYP3A4 compared with CYP3A5 and CYP3A7, it was not as selective for CYP3A4 compared with CYP3cide; IC<sub>50</sub> values for CYP3cide with CYP3A4 were ~1000-fold lower compared with CYP3A7, and in comparison, azamulin CYP3A4 IC<sub>50</sub> values varied between 10 and 100-fold lower than CYP3A7 depending on the probe selection. Azamulin also could not be used to distinguish between CYP3A5 and CYP3A7 activity without also inhibiting CYP3A7 due to azamulin's similar specificity for these CYP3A isoforms. The CYP3cide and CP concentrations tested (1 μM and 0.5 μM, respectively) were selected to be at least 5 times the IC<sub>50</sub> value of the corresponding specific P450 isoform but low enough to limit potential inhibition of CYP3A7. Under these conditions, the 16α-OH-DHEA metabolite is highly representative of CYP3A7 activity. At the concentrations used, CYP3cide had minimal effects on CYP3A7 activity across all DHEA metabolites measured (Fig. 5). The formation of 16α-OH-DHEA, the main metabolite formed by CYP3A7, was inhibited by CYP3cide by ~8% compared with the solvent control when CYP3A7 was the only P450 enzyme present; however, when CYP3A4 and CYP3A7 were both present in the reaction, 16α-OH-DHEA formation levels matched CYP3A7 control levels, likely due to CYP3cide's preference toward CYP3A4. CYP3A4 alone was inhibited by ~84% (data not shown), whereas CYP3A7 activity was minimal (Fig. 5A). The same pattern was observed for metabolite formation of 7β-OH- and 7α-OH-DHEA, both minor metabolites of DHEA metabolism produced by CYP3A7; for these metabolites, CYP3A7 was only inhibited by ~5% compared with the solvent control and unaffected when in solution with CYP3A4 (Fig. 5, B and C).

CP inhibited CYP3A7 DHEA metabolism by 12%–16% when no other P450 enzyme was in the reaction (Fig. 5, A–C). In reactions where CYP3A5 and CYP3A7 were present, CYP3A5 did not significantly increase DHEA metabolism; if we assume that CP inhibited 100% of DHEA metabolism by CYP3A5 and the only formation observed is from CYP3A7 activity, CP appears to be inhibiting ~15% of 16α-OH-DHEA formation by CYP3A7 (Fig. 5A). The same pattern is observed when measuring 7α-OH-DHEA formation (Fig. 5C). Although formation of 7β-OH-DHEA was detectable across all reactions, CP inhibited CYP3A5 and CYP3A7 activity to concentration levels below the level of quantification (Fig. 5B).

In solvent control reaction mixtures containing equal amounts of CYP3A4, CYP3A5, and CYP3A7, the total formation of all three metabolites decreased compared with solvent control reactions only containing CYP3A4 and CYP3A7; this is likely due to the similar K<sub>m</sub> values of DHEA and competitive binding between the three isoforms. Thus, DHEA is distributed between the CYP3A enzymes and lowering the overall observed metabolism. The effects of CYP3cide are similar to those observed in CYP3A4/7 reaction mixtures; CYP3A4 activity is ~85% inhibited, and CYP3A7 activity is not significantly reduced (<5% inhibition). Interestingly, CP effects were not as inhibitory toward CYP3A7 when in the presence of CYP3A4 and CYP3A5; CYP3A7 activity only decreased by 5%–10% compared with the CYP3A7 solvent control (Fig. 5A). Similar to DHEA, this could be due to CP competing for binding between all the CYP3A isoforms. CP appears to show more preference for CYP3A5 and CYP3A4 than CYP3A7 in mixed solutions. The off-target effects of CP are reduced depending on the ratio of CYP3A enzymes present.



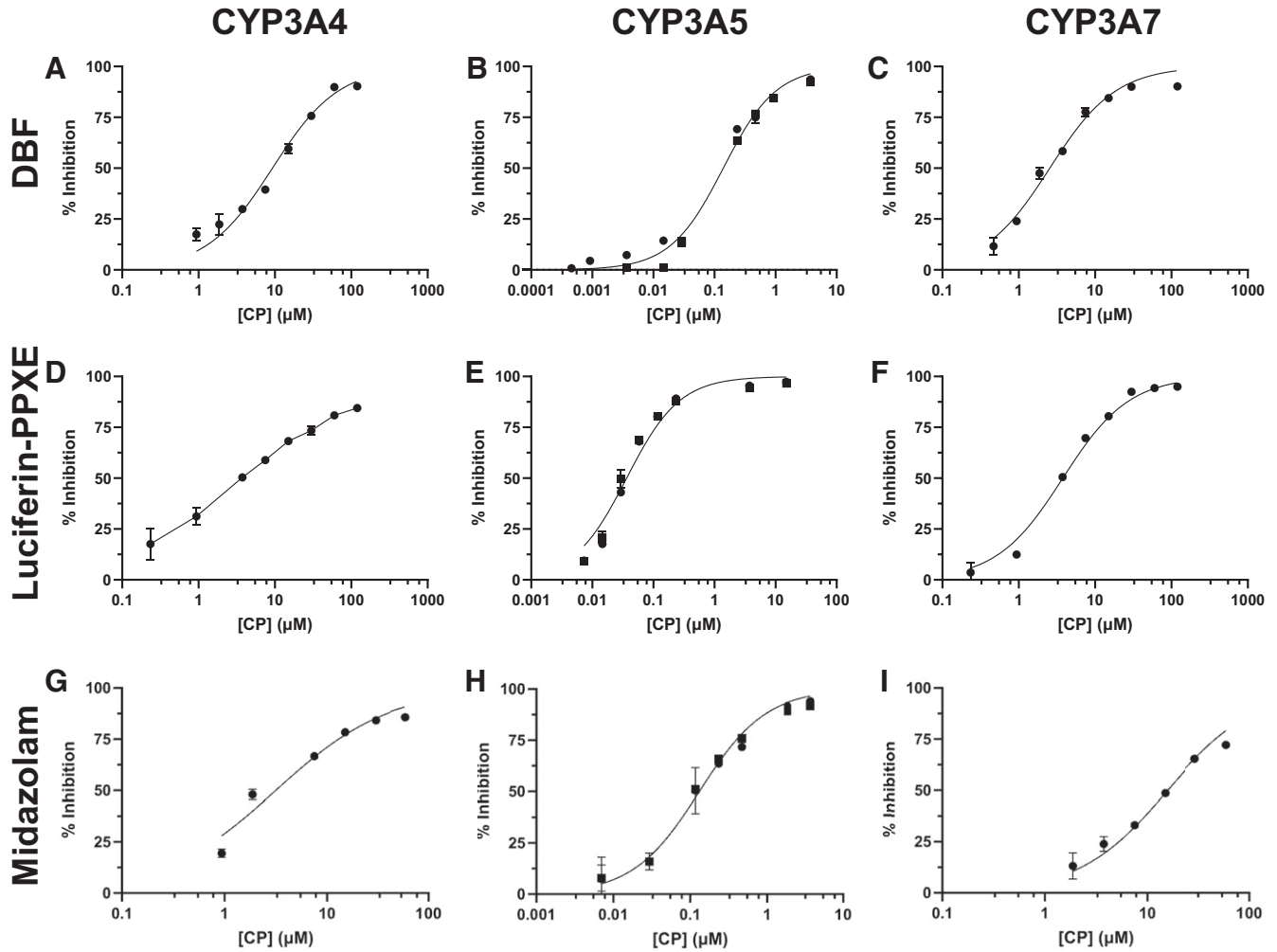


**Fig. 3.** CYP3A4, CYP3A5, and CYP3A7 selectivity for clobetasol propionate inhibition using dibenzylfluorescein (A–C), luciferin-PPXE (D–F), and midazolam (G–I) as probes. Data points represent the average of triplicate incubations, with error bars representing the standard deviations. Filled circles, 30-minute preincubation in the absence of NADPH; closed squares, 30-minute preincubation in the presence of NADPH. All curves were generated as described in *Materials and Methods*, except for CYP3A4/Luciferin-PPXE (D) and CYP3A4/Midazolam (G), which were generated using a different nonlinear regression model [(Inhibitor) versus response—variable slope (four parameters)] in GraphPad Prism (version 10.2.0).

### Discussion

The incidence of off-label medicines prescribed and administered in the NICU population varies from 34% to 100% due to the fact that the majority of drugs are tested for safety and efficacy only in the general adult population and not in neonates. This high rate of off-label drug use has, in turn, caused a high incidence rate of DDIs in neonates. In a recent cohort study of 220 NICU patients, 70% experienced a DDI incident, almost 30% of which included major adverse reactions, such as respiratory depression (Costa et al., 2021). The risk for metabolism-based DDIs is most commonly assessed with pooled adult HLMs. However, drug dosing and safety in neonates is often determined by extrapolating from the dosing regimens validated in other pediatric and adult cohorts and rarely incorporates neonatal physiology.

To better estimate drug safety in neonates, preclinical drug testing ideally would be performed using nHLMs; however, these are a rare resource and often not commercially available. As an alternative, characterizing CYP3A7 enzyme activity in nHLMs and obtaining an intersystem extrapolation factor for use with recombinant enzyme could be a plausible solution to estimate relative rates of drug metabolism and enzyme inhibition for drugs that are primarily metabolized through the CYP3A pathway. Although neonates principally express

CYP3A7 in the liver, they also may have low levels of CYP3A4 and CYP3A5. These three enzymes have similar affinities to drugs, which makes it difficult to differentiate the activity of these enzymes when they are present simultaneously. To distinguish CYP3A7 activity, we investigated the use of three recently reported CYP3A inhibitors—CYP3cide, clobetasol propionate, and azamulin. To this end, we tested a variety of probes ranging in sensitivity and ease of detection as probe selection has previously been shown to influence levels of enzyme inhibition. DBF is a CYP3A fluorescent substrate routinely used as a probe for CYP3A activity. Luciferin-PPXE is part of an enzyme assay kit sold by Promega (P450-Glo), is DMSO tolerant, and is commonly used as a CYP3A4 high-throughput screening probe. Midazolam is a standard CYP3A probe, both sensitive and biologically relevant, as midazolam is administered both to neonates and adults for anesthesia.

We conducted inhibition experiments using the nondilution method over the more commonly employed dilution method to assess metabolism-dependent inhibition (Parkinson et al., 2011). There is substantial variation in the literature reports, and between individual research groups, regarding whether the  $IC_{50}$  shift is deduced from the predilution or postdilution concentration when using the dilution method. When

TABLE 2  
CP IC<sub>50</sub> shift for the CYP3A4, CYP3A5, and CYP3A7 recombinant enzymes

| Probe Substrate | Clobetazol propionate IC <sub>50</sub> (μM) (95% CI) [R <sup>2</sup> ] |                             |                |                                      |                               |            |
|-----------------|--|-----------------------------|----------------|--------------------------------------|-------------------------------|------------|
|                 | DBF  |                             | Luciferin-PPXE |                                      | Midazolam                     |            |
|                 | -NADPH preincubation   | +NADPH preincubation        | Fold shift     | -NADPH preincubation                 | +NADPH preincubation          | Fold shift |
| CYP3A4          | 9.29 (7.36–11.7) [0.98]  | N/A                         | N/A            | 3.16 (1.61–4.40) [0.99] <sup>f</sup> | N/A                           | N/A        |
| CYP3A5          | 0.157 (0.121–0.202) [0.99]   | 0.115 (0.0811–0.158) [0.99] | 1.37           | 0.0382 (0.0287–0.0508) [0.97]        | 0.0349 (0.0264–0.0461) [0.97] | 1.09       |
| CYP3A7          | 2.55 (0.216–0.496) [0.98]  | N/A                         | N/A            | 3.78 (3.12–4.57) [0.99]              | N/A                           | N/A        |
|                 |  |                             |                | -NADPH preincubation                 | +NADPH preincubation          | Fold shift |
|                 |  |                             |                | 3.16 (1.75–5.22) [0.95] <sup>f</sup> | 0.135 (0.105–0.172) [0.99]    | N/A        |
|                 |  |                             |                | 0.128 (0.103–0.158) [0.99]           | N/A                           | 0.948      |
|                 |  |                             |                | 15.8 (12.7–19.8) [0.97]              | N/A                           | N/A        |

N/A, not applicable.

<sup>f</sup>Fit with the variable Hill Slope equation with a HillSlope value of 0.584.

<sup>g</sup>Fit with the variable Hill Slope equation with a HillSlope value of -0.778.

processed on the final or postdilution inhibitor concentration, IC<sub>50</sub> values typically decrease by the magnitude of the dilution factor. Additionally, the dilution method requires using a high amount of enzyme, which can lead to free inhibitor depletion due to nonspecific binding. These considerations led us to choose the nondilution approach.

The results we obtained are in agreement with previous findings regarding CYP3A4 specificity for CYP3A4 (Walsky et al., 2012), even though our probe substrates varied from those previously studied (testosterone and midazolam). CYP3A4 was found to be an irreversible inhibitor of only CYP3A4, with an IC<sub>50</sub> value three orders of magnitude lower than CYP3A5 and CYP3A7 across all probe substrates tested. Testing metabolism-dependent inhibition of CYP3A4 by CYP3A4 using midazolam as a probe resulted in an IC<sub>50</sub> value 10-fold lower than that obtained by DBF and luciferin-PPXE. Midazolam, as a substrate probe of enzyme activity, is more specific for CYP3A4 and requires either a liquid chromatography or LC-MS assay, lending additional credence to the results obtained with this probe substrate.

Although CP was most specific for CYP3A5, it did not exhibit an NADPH dependence as would be indicative of an MDI. Previous work suggests CP to be a heme-mediated inhibitor based on differences in drug-induced Soret spectral shifts between CYP3A4 and CYP3A5 as well as an in silico docking/molecular dynamics study (Wright et al., 2020). However, none of the seven criteria for definitive MDI identification were satisfied in this study (Silverman, 1995) nor were inactivation constant (K<sub>i</sub>) and activation rate (K<sub>inact</sub>) determined. Moreover, the IC<sub>50</sub> shift experiments conducted in this paper do not support this claim as no shift was identified with recombinant P450 enzyme. In regard to P450 MDI determination, Soret spectra and in silico docking/molecular dynamics can be misleading, which underscores the importance of Silverman's seven criteria for definitive MDI determination. It is possible that the inactivation is not dependent on metabolism and that CP may simply be a tightly bound competitive inhibitor.

The IC<sub>50</sub> values reported for CYP3A4 and CYP3A5 were 15.6 μM and 0.206 μM, respectively, based upon activity assays using luciferin-IPA as a probe substrate (Wright et al., 2020). Across all three probe substrates we tested, no IC<sub>50</sub> values obtained were in the same range for CYP3A4 as the value previously reported by Wright et al. (2020), signifying the importance of probe selection in P450 inhibition assays. CYP3A4 and CYP3A7 had comparable IC<sub>50</sub> values for CP across all probe substrates, with the exception of CYP3A7 testing with midazolam, which resulted in an IC<sub>50</sub> value more than 10-fold greater than that of CYP3A4. CYP3A7 activity was tested well below the K<sub>m</sub> value of midazolam (15 μM versus ~115 μM), which potentially distorted the results. Furthermore, CYP3A4 inhibition by CP suggested negative cooperativity as evidenced through its activity with midazolam and luciferin-PPXE (Fig. 3; Table 2). The resulting Hill coefficient for midazolam and luciferin-PPXE testing were -0.778 and 0.584, respectively. Due to CP's structure, it is not entirely surprising that this compound had the lowest specificity for any of the CYP3A enzymes. The structure is comprised of the basic steroid skeleton, and CYP3A enzymes are well known to metabolize endogenous steroids as well as play a significant role in their synthesis (e.g., testosterone, estrogen, dehydroepiandrosterone, etc.). This greatly explains all three enzymes' capacity to interact with this compound.

Across all three inhibitors, testing CYP3A5 inhibition with luciferin-PPXE as an activity probe resulted in values that were significantly less than the values generated with midazolam and DBF. This is likely due to the poor metabolizing capabilities of CYP3A5 in regard to luciferin-PPXE. No commercially available luciferin substrate is

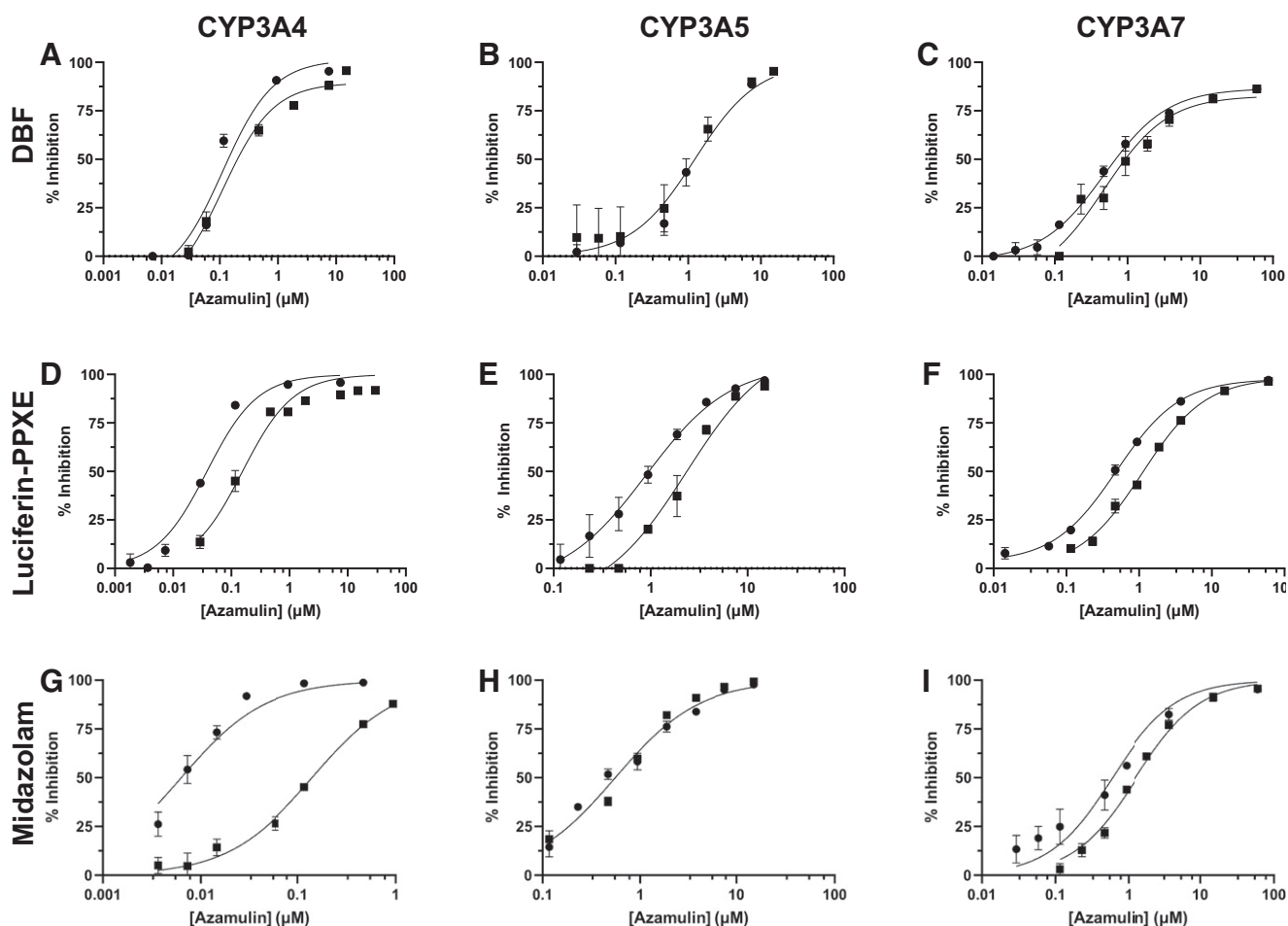


**Fig. 4.** CYP3A4, CYP3A5, and CYP3A7 selectivity for azamulin inhibition using dibenzylfluorescein (A–C), luciferin-PPXE (D–F), and midazolam (G–I) as probes. Data points represent the average of triplicate incubations, with error bars representing the standard deviations. Filled circles, 30-minute preincubation in the presence of NADPH; closed squares, 30-minute preincubation in the absence of NADPH. All curves were generated as described in *Materials and Methods*.

recommended specifically for CYP3A5; those indicated for CYP3A4 can also be used to assay CYP3A5 or CYP3A7, according to the manufacturer (Promega). Although it would have been preferred to use luciferin-IPA for easier comparison with Wright et al. (2020), this probe is DMSO intolerant, which we found problematic since the inhibitors and DHEA probe are dissolved in this solvent. Therefore, Luciferin-PPXE was chosen instead because of its DMSO solubility when compared with the other luciferin products and its selectivity for the CYP3A enzymes. However, our data show that choosing this probe can compromise the results obtained with CYP3A5. Interestingly, of all the enzymes tested, CYP3A5 seemed most sensitive to substrate probe selection.

Azamulin was previously reported to be a CYP3A4/5 inhibitor based upon incubation with hepatocytes (Chanteux et al., 2020). However, the degree of its specificity varied between the probes used. For instance, incubations with DBF produced  $IC_{50}$  values within the same range for CYP3A4 and CYP3A7, whereas midazolam produced  $IC_{50}$  values with a 20-fold difference between CYP3A4 and CYP3A7. Interestingly, azamulin was also found to be an MDI of CYP3A4 and CYP3A7 but not CYP3A5 across all probe substrates tested. CYP3A4 and CYP3A7 have the highest sequence identity between these three CYP3A enzymes (~88%), which may help explain the similar results obtained with these enzymes.

Although probe selection did not seem to influence  $IC_{50}$  values, it did have a drastic effect on the metabolism-dependent  $IC_{50}$  values. Even

though all three inhibitors examined displayed various affinities to the respective CYP3A enzymes, in all cases the most significant  $IC_{50}$  shifts occurred with midazolam as a probe substrate. This suggests that midazolam metabolism may be more sensitive to MDI than other probe substrates.

CYP3Cide and CP were evaluated further and were found to be promising inhibitors for the purpose of probing CYP3A7 activity in nHLMs. The abundance of CYP3A5 in fetal and neonatal samples has been reported to be significantly lower or nonexistent compared with CYP3A7 (Hakkola et al., 2001; Fanni et al., 2014). Thus, it is not as integral to have a specific inhibitor of CYP3A5 in most nHLMs studies. Despite this consideration, at low concentrations CP is a promising inhibitor to minimize CYP3A5 activity without disturbing CYP3A7.

In contrast to CYP3A5, CYP3A4 abundance has been reported to increase after ~2 weeks postnatal age and can reach 30%–40% of adult values by 4 weeks of age (Hines 2007; O'Hara et al., 2015). However, the onset of CYP3A4 development can be delayed due to premature birth, causing high interindividual variation. Thus, being able to differentiate between CYP3A4 and CYP3A7 is critical for assessing CYP3A7's contribution to the metabolism of any particular drug. In conclusion, our results signify CYP3Cide and CP's ability to inhibit CYP3A4 and CYP3A5 without significantly disrupting CYP3A7 activity in systems with mixed CYP3A enzymes, thus providing an important tool to assay



TABLE 3  
Azamulin IC<sub>50</sub> shift for the CYP3A4, CYP3A5, and CYP3A7 recombinant enzymes

| Probe Substrate | DBF                         |            | Luciferin-PPXE             |            | Midazolam                         |            |
|-----------------|-----------------------------|------------|----------------------------|------------|-----------------------------------|------------|
|                 | -NADPH preincubation        | Fold shift | -NADPH preincubation       | Fold shift | -NADPH preincubation              | Fold shift |
| CYP3A4          | 0.171 (0.0368–0.489) [0.99] | 1.64       | 0.156 (0.102–0.236) [0.95] | 2.72       | 0.00112 (0.000632–0.00187) [0.83] | 52.2       |
| CYP3A5          | 1.07 (0.795–1.43) [0.99]    | 0.75       | 2.34 (1.05–5.34) [0.98]    | 2.60       | 0.534 (0.436–0.654) [0.98]        | 1.09       |
| CYP3A7          | 0.614 (0.149–1.83) [0.96]   | 1.44       | 1.10 (0.843–1.43) [0.99]   | 2.23       | 0.605 (0.385–0.948) [0.96]        | 2.17       |

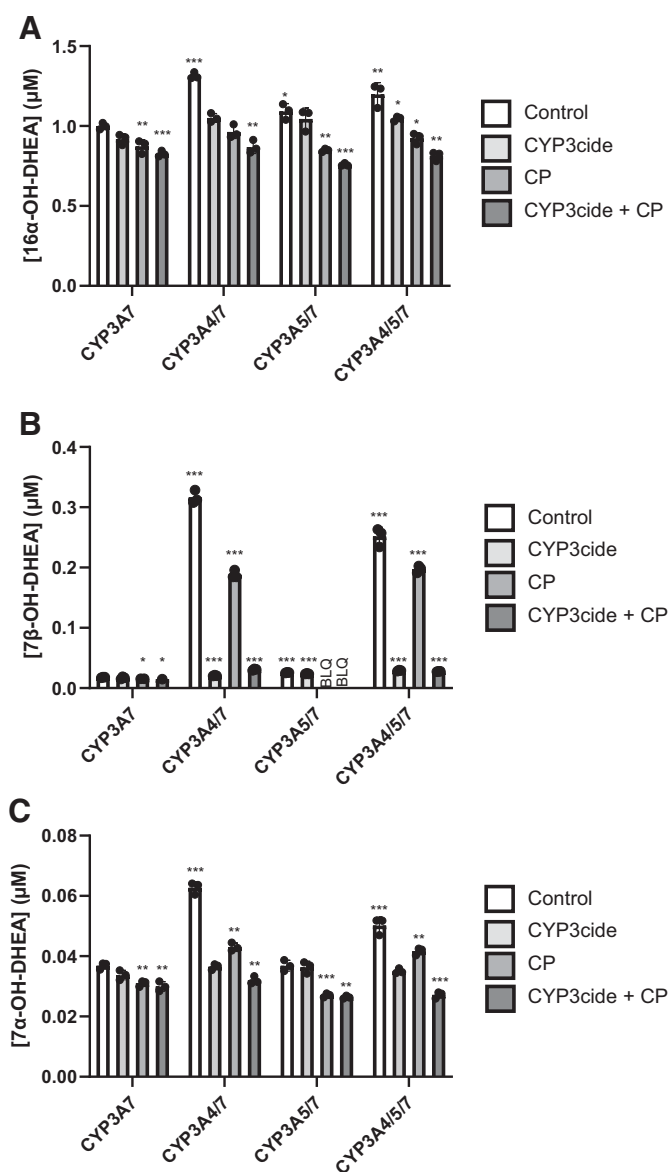


**Fig. 5.** DHEA hydroxylation to (A) 16 $\alpha$ -OH-, (B) 7 $\beta$ -OH-, and (C) 7 $\alpha$ -OH-DHEA by various rCYP3A mixtures and inhibition by CYP3cide and CP. Data points represent individual measurements from a single incubation, whereas the bars represent the average of the three data points, with error bars representing the standard deviations. Some measurements were below the level of quantification (BLQ) and are not shown (B). Groups were compared with the CYP3A7 solvent control for statistical significance using Welch's *t* test. \**P* < 0.05; \*\**P* < 0.01; \*\*\**P* < 0.001.

for the specific contribution of CYP3A7 to the metabolism of individual drugs.

#### Data Availability

The authors declare that all the data supporting the findings of this study are contained within the paper.

#### Authorship Contributions

*Participated in research design:* Work, Kandel, Lampe.

*Conducted experiments:* Work.

*Performed data analysis:* Work.

*Wrote or contributed to the writing of the manuscript:* Work, Kandel, Lampe.

## References

- Chanteux H, Rosa M, Delatour C, Nicolai J, Gillent E, Dell'Aiera S, and Ungell A-L (2020) Application of Azamulin to Determine the Contribution of CYP3A4/5 to Drug Metabolic Clearance Using Human Hepatocytes. *Drug Metab Dispos* **48**:778–787.
- Costa HT, Leopoldino RWD, da Costa TX, Oliveira AG, and Martins RR (2021) Drug-drug interactions in neonatal intensive care: A prospective cohort study. *Pediatr Neonatol* **62**:151–157.
- Fabiano V, Mameli C, and Zuccotti GV (2012) Adverse drug reactions in newborns, infants and toddlers: pediatric pharmacovigilance between present and future. *Expert Opin Drug Saf* **11**:95–105.
- Fanni D, Ambu R, Gerosa C, Nemolato S, Castagnola M, Van Eyken P, Faa G, and Fanos V (2014) Cytochrome P450 genetic polymorphism in neonatal drug metabolism: role and practical consequences towards a new drug culture in neonatology. *Int J Immunopathol Pharmacol* **27**:5–13.
- Hakkola J, Raunio H, Purkunen R, Saarikoski S, Vähäkangas K, Pelkonen O, Edwards RJ, Boobis AR, and Pasanen M (2001) Cytochrome P450 3A expression in the human fetal liver: evidence that CYP3A5 is expressed in only a limited number of fetal livers. *Biol Neonate* **80**:193–201.
- Hines RN (2007) Ontogeny of human hepatic cytochromes P450. *J Biochem Mol Toxicol* **21**:169–175.
- Leeder JS, Gaedigk R, Marcucci KA, Gaedigk A, Vyhlihal CA, Schindel BP, and Pearce RE (2005) Variability of CYP3A7 expression in human fetal liver. *J Pharmacol Exp Ther* **314**:626–635.
- Li H and Lampe JN (2019) Neonatal cytochrome P450 CYP3A7: A comprehensive review of its role in development, disease, and xenobiotic metabolism. *Arch Biochem Biophys* **673**:108078.
- Maldonado AQ, Asempa T, Hudson S, and Rebellato LM (2017) Prevalence of CYP3A5 Genomic Variants and Their Impact on Tacrolimus Dosing Requirements among Kidney Transplant Recipients in Eastern North Carolina. *Pharmacotherapy: The Journal of Human Pharmacology and Drug Therapy* **37**:1081–1088.
- Morselli PL, Franco-Morselli R, and Bossi L (1980) Clinical pharmacokinetics in newborns and infants. Age-related differences and therapeutic implications. *Clin Pharmacokinet* **5**:485–527.
- O'Hara K, Wright IMR, Schneider JJ, Jones AL, and Martin JH (2015) Pharmacokinetics in neonatal prescribing: evidence base, paradigms and the future. *Br J Clin Pharmacol* **80**:1281–1288.
- Pacifici GM (2015) Clinical pharmacology of fentanyl in preterm infants. A review. *Pediatr Neonatol* **56**:143–148.
- Parkinson A, Kazmi F, Buckley DB, Yerino P, Paris BL, Holsapple J, Toren P, Otradovec SM, and Ogilvie BW (2011) An evaluation of the dilution method for identifying metabolism-dependent inhibitors of cytochrome P450 enzymes. *Drug Metab Dispos* **39**:1370–1387.
- Shankar K and Mehendale HM (2014) Cytochrome P450, in *Encyclopedia of Toxicology* (Wexler P, ed) vol 3, pp 1125–1127, Oxford: Academic Press, Oxford, England.
- Silverman RB (1995) Mechanism-based enzyme inactivators, in *Methods in Enzymology* vol 249, pp 240–283, Academic Press, Oxford, England.
- Stewart CF and Hampton EM (1987) Effect of maturation on drug disposition in pediatric patients. *Clin Pharm* **6**:548–564.
- Van den Anker JN, McCune S, Annaert P, Baer GR, Mulugeta Y, Abdelrahman R, Wu K, Krudys KM, Fisher J, Slikker W, et al. (2020) Approaches to Dose Finding in Neonates, Illustrating the Variability between Neonatal Drug Development Programs. *Pharmaceutics* **12**:685.
- Walsky RL, Obach RS, Hyland R, Kang P, Zhou S, West M, Geoghegan KF, Helal CJ, Walker GS, Goosen TC, et al. (2012) Selective mechanism-based inactivation of CYP3A4 by CYP3Cide (PF-04981517) and its utility as an in vitro tool for delineating the relative roles of CYP3A4 versus CYP3A5 in the metabolism of drugs. *Drug Metab Dispos* **40**:1686–1697.
- Williams JA, Ring BJ, Cantrell VE, Jones DR, Eckstein J, Ruterbories K, Hamman MA, Hall SD, and Wrighton SA (2002) Comparative metabolic capabilities of CYP3A4, CYP3A5, and CYP3A7. *Drug Metab Dispos* **30**:883–891.
- Wright WC, Cheng J, Wang J, Girvan HM, Yang L, Chai SC, Huber AD, Wu J, Oladimeji PO, Munro AW, et al. (2020) Clobetasol Propionate Is a Heme-Mediated Selective Inhibitor of Human Cytochrome P450 3A5. *J Med Chem* **63**:1415–1433.
- Zane NR, Chen Y, Wang MZ, and Thakker DR (2018) Cytochrome P450 and flavin-containing monooxygenase families: age-dependent differences in expression and functional activity. *Pediatr Res* **83**:527–535.

---

**Address correspondence to:** Dr. Jed N. Lampe, Department of Pharmaceutical Sciences University of Colorado, Skaggs School of Pharmacy and Pharmaceutical Sciences, 12850 E. Montview Boulevard, V20-2108, Aurora, CO 80045. E-mail: jed.lampe@cuanschutz.edu

---

## Supplemental Data for

“Comparison of the CYP3A selective inhibitors  
CYP3cide, clobetasol, and azamulin for their  
potential to distinguish CYP3A7 activity in the  
presence of CYP3A4/5”

*Hannah M. Work, Sylvie E. Kandel, and Jed N. Lampe\**

Department of Pharmaceutical Sciences, Skaggs School of Pharmacy, University of Colorado,  
Aurora, Colorado 80045, United States.

## Supplemental Data

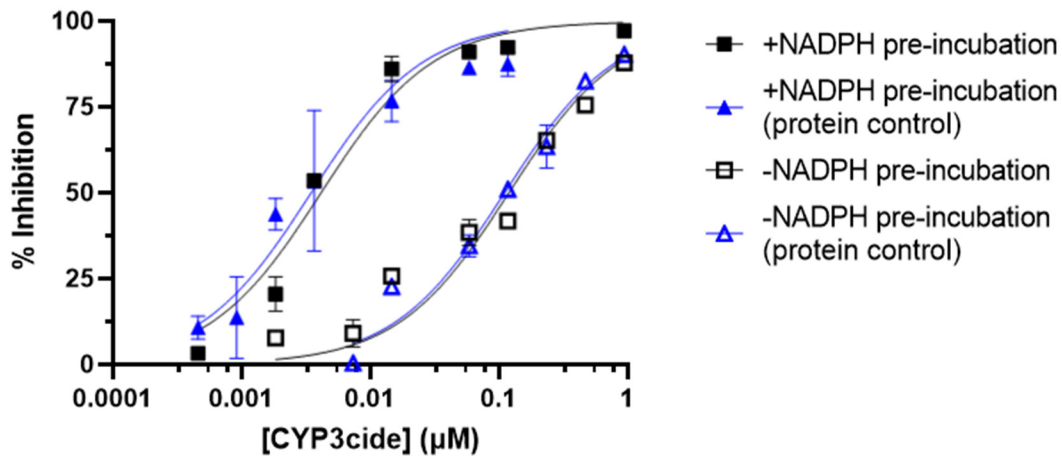


**Figure S1: Effect of differing protein content on CYP3cide binding to CYP3A4 measuring using midazolam as a probe substrate.** Black data points represent experiments at 2 pmol/mL CYP3A4, and blue data points represent experiments at 10 pmol/mL CYP3A4. All data points represent the average of triplicate incubations, with error bars representing the standard deviations. Curves were generated as described in the Methods section.

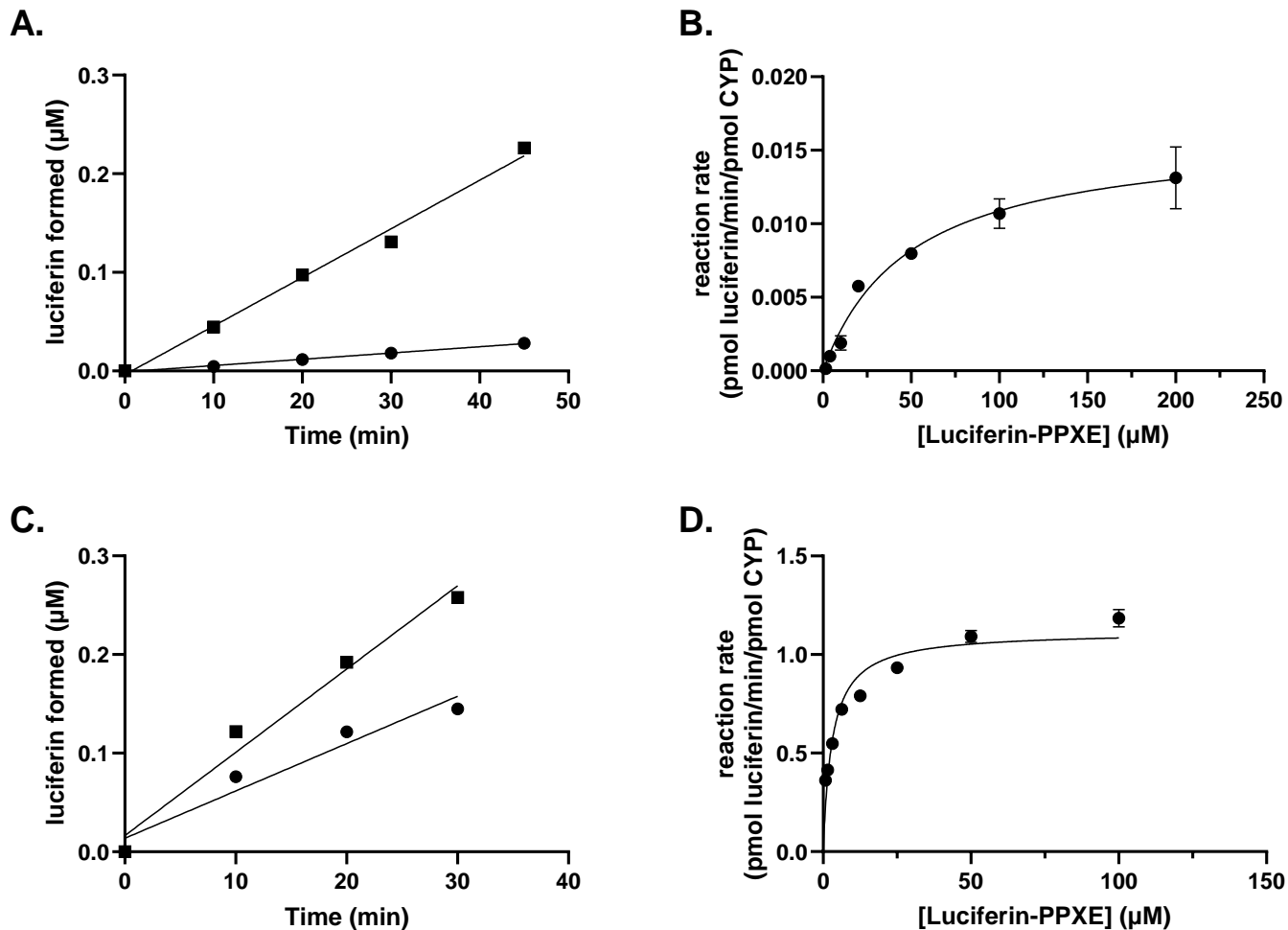


**Figure S.2: Luciferin formation linearity and  $K_m/V_{max}$  characterization for CYP3A5 (A,B) and CYP3A7 (C,D).** All points represent the average of duplicate values. CYP3A5 and CYP3A7 experiments were performed using 20 pmol/ml and 10 pmol/ml enzyme in reactions, respectively. The black squares and circles in panels A and C represent experiments using 50  $\mu\text{M}$  and 5  $\mu\text{M}$  luciferin-PPXE concentrations, respectively. The resulting  $K_m$  values for CYP3A5 and CYP3A7 were 49  $\mu\text{M}$  and 3  $\mu\text{M}$ , respectively.



**Table S1: Incubation parameters for CYP3A4, CYP3A5, and CYP3A7 recombinant assays using the probe substrates DBF, luciferin-PPXE, and midazolam.**

| Probe substrate                   | Dibenzylfluorescein |      |      | Luciferin-PPXE |     |     | Midazolam |     |     |
|-----------------------------------|---------------------|------|------|----------------|-----|-----|-----------|-----|-----|
|                                   | 3A4                 | 3A5  | 3A7  | 3A4            | 3A5 | 3A7 | 3A4       | 3A5 | 3A7 |
| CYP isoform                       |                     |      |      |                |     |     |           |     |     |
| [Substrate] ( $\mu\text{M}$ )     | 0.15                | 0.15 | 0.15 | 25             | 25  | 2.5 | 1.5       | 1.5 | 15  |
| [Enzyme] (pmol/ml)                | 10                  | 10   | 10   | 10             | 20  | 10  | 2         | 2   | 10  |
| Incubation time (min)             | 15                  | 15   | 15   | 15             | 30  | 15  | 4         | 4   | 30  |
| Reaction volume ( $\mu\text{l}$ ) | 100                 | 100  | 100  | 50             | 50  | 50  | 200       | 200 | 200 |